Research Square

Preprints are preliminary reports that have not undergone peer review.
They should not be considered conclusive, used to inform clinical practice,
or referenced by the media as validated information.

Performance Analysis of a Low-Complexity Hybrid DF–SIR Protocol for Coded Cooperative Hybrid Satellite–Terrestrial Networks

Slim Chaoui

schaoui@ju.edu.sa

Jouf University

Research Article

Keywords:

Posted Date: November 4th, 2026

DOI: https://doi.org/10.21203/rs.3.rs-11411957/v1

License: This work is licensed under a Creative Commons Attribution 4.0 International License.
Read Full License

Additional Declarations: No competing interests reported.

Performance Analysis of a Low-Complexity Hybrid DF–SIR Protocol for Coded Cooperative Hybrid Satellite–Terrestrial Networks

Slim Chaoui[1*]

[1]Department of Computer Engineering and Networks, College of Computer and Information Sciences, Jouf University, Sakaka, 72388, Saudi Arabia.

Corresponding author(s). E-mail(s): schaoui@ju.edu.sa;

Abstract

Hybrid satellite-terrestrial cooperative networks (HSTCNs) are a key enabler of sixth-generation (6G) non-terrestrial networks, providing resilient wide-area coverage under heterogeneous propagation conditions. This paper proposes a low-complexity hybrid decode-and-forward and soft-information-relaying (HDF-SIR) protocol for coded cooperative HSTCNs operating over mixed satellite-terrestrial fading channels. In the proposed scheme, each relay adaptively switches between decode-and-forward (DF) and soft-information-relaying (SIR) modes according to its decoding reliability, allowing unreliable relays to forward reliability-weighted soft symbols instead of being excluded from cooperation. The satellite-relay and satellite-destination links are modeled by shadowed-Rician fading, while the relay-destination hop follows a Nakagami-$\boldsymbol{m}$ distribution, capturing both satellite shadowing effects and terrestrial channel variability. To enable analytical tractability, a moment-based statistical model is developed for the soft symbols generated at the output of the relay's soft-input soft-output decoder, leading to an equivalent soft-channel representation. Based on this model, closed-form and semi-analytical expressions are derived for the end-to-end signal-to-noise ratio (SNR), outage probability, and symbol error rate (SER) with opportunistic relay selection. Monte Carlo simulations validate the analysis and demonstrate that the proposed hybrid DF-SIR protocol preserves cooperative diversity while significantly improving reliability compared with conventional DF-only and SIR-only relaying, particularly in the mid-SNR regime where decoding reliability is uncertain. Owing to its direct reuse of decoder-generated log-likelihood ratios without additional re-encoding or iterative processing, the proposed scheme achieves a favorable performance-complexity trade-off, making

it a practical and energy-efficient solution for future 6G hybrid satellite-terrestrial communication systems.

Keywords: Hybrid satellite-terrestrial networks, soft-information relaying, mixed Rician-Nakagami fading, 6G non-terrestrial networks.

1 Introduction

The integration of satellite and terrestrial networks is a cornerstone of sixth-generation (6G) non-terrestrial networks (NTN), aiming to provide seamless global connectivity, resilient coverage, and service continuity in areas where terrestrial infrastructure is unavailable, unreliable, or temporarily disrupted. Hybrid satellite–terrestrial communication networks (HSTCNs) exploit the complementary characteristics of satellite links and terrestrial access networks to enhance coverage and reliability in challenging propagation environments [1–3]. However, the performance of HSTCNs is fundamentally limited by severe and heterogeneous channel impairments, including shadowing and intermittent line-of-sight (LoS) conditions on satellite links and rapidly varying fading on terrestrial hops, which jointly degrade end-to-end reliability.

To combat these impairments, cooperative relaying has been widely adopted in HSTCNs, where terrestrial relays assist the satellite in forwarding information to shadowed or cell-edge users [4–7]. The effectiveness of such cooperative architectures critically depends on the relaying strategy employed between the satellite, relays, and destination. Classical amplify-and-forward (AF) relaying offers low implementation complexity but inevitably amplifies noise, while decode-and-forward (DF) relaying eliminates noise at the relay at the cost of assuming reliable decoding. In practical fading conditions, decoding errors at the relay are unavoidable, and erroneous hard decisions lead to severe error propagation. To mitigate this effect, most DF-based schemes restrict cooperation to relays that decode successfully, which in turn reduces cooperative diversity and degrades performance when decoding reliability fluctuates across relays [8–10]. Recent developments have also examined hybrid relaying. Zhou *et al.* [11] and Wang *et al.* [12] analyzed hybrid DF-AF networks integrated with energy harvesting techniques, highlighting how energy-aware relay switching can improve reliability and energy efficiency. Liu *et al.* [13], Wu *et al.* [14], and Tang and Zhao [15] investigated hybrid DF-AF relaying combined with distributed space time codes, demonstrating its potential to improve diversity and robustness against channel fading.

Although hybrid satellite-terrestrial networks have been analyzed extensively with AF, DF, and AF/DF strategies [3, 10, 16], none of these studies have yet incorporated soft information relaying (SIR) in the hybrid context. Existing analyses either assume hard-decision forwarding or restrict cooperation to correctly decoded relays, which limits its diversity gain and spectral efficiency. Soft-information relaying, originally proposed for terrestrial cooperative networks, allows relays to forward reliability-weighted soft symbols or log-likelihood ratios (LLRs) instead of hard decisions, thereby mitigating error propagation while preserving cooperative diversity [17]. Despite its proven benefits in terrestrial systems, SIR has not yet been investigated in the context of hybrid

satellite–terrestrial cooperative networks. Extending SIR to HSTCNs is non-trivial due to the mixed nature of the underlying channels, where satellite links typically follow shadowed-Rician statistics while terrestrial relay–destination links are more accurately modeled by Rayleigh or Nakagami-m fading [18–20].

This paper addresses this gap by proposing a hybrid decode-and-forward and soft-information-relaying (HDFSIR) framework for coded cooperative HSTCNs. In the proposed scheme, each relay dynamically switches between DF and SIR modes according to its decoding reliability, enabling reliable relays to forward clean codewords while allowing unreliable relays to contribute soft reliability information instead of being silenced. Unlike existing HSTCN relaying schemes that rely on hard-decision AF or DF forwarding [4, 5, 7, 8, 10, 21], the proposed HDFSIR framework exploits decoder-generated soft information, allowing unreliable relays to contribute to cooperation instead of being excluded. To enable analytical tractability under mixed fading conditions, we introduce a moment-based statistical model for the soft symbols produced at the output of the relay's soft-input soft-output (SISO) decoder, which captures the impact of shadowed-Rician satellite links on the effective relay output.

Based on the proposed soft-channel model, closed-form and semi-analytical expressions are derived for the instantaneous end-to-end signal-to-noise ratio (SNR), outage probability, and symbol error rate (SER) of opportunistic HDFSIR relaying over mixed shadowed-Rician and Nakagami-m fading channels. The proposed framework preserves cooperative diversity while significantly mitigating error propagation in the mid-SNR regime where decoding reliability is uncertain. These properties make HDFSIR relaying particularly well suited for energy- and complexity-constrained 6G NTN scenarios, such as satellite-assisted IoT access, UAV-supported coverage extension, and resilient broadband connectivity in obstructed or disaster-affected environments.

The main contributions of this paper are summarized as follows:

- We propose, for the first time, a HDFSIR framework for hybrid satellite–terrestrial cooperative networks. By enabling each relay to dynamically switch between DF and SIR modes according to its decoding reliability, the proposed scheme effectively mitigates error propagation while preserving cooperative diversity in multi-relay scenarios.
- We develop a moment-based statistical model for the soft symbols generated at the output of the relay's SISO decoder under shadowed-Rician satellite fading. The proposed model yields an equivalent soft-channel representation that enables tractable performance analysis in hybrid satellite–terrestrial environments.
- Leveraging the derived soft-channel statistics, we obtain closed-form and semi-analytical expressions for the end-to-end SNR, outage probability, and SER of the proposed HDFSIR scheme over mixed shadowed-Rician and Nakagami-m fading channels.
- We analyze the computational efficiency of the proposed HDFSIR strategy and show that its SIR mode directly exploits decoder-generated LLRs without requiring re-encoding or iterative processing. This feature provides a favorable performance–complexity trade-off, making the scheme suitable for energy- and processing-constrained relays such as UAV-assisted nodes and satellite-enabled IoT devices.

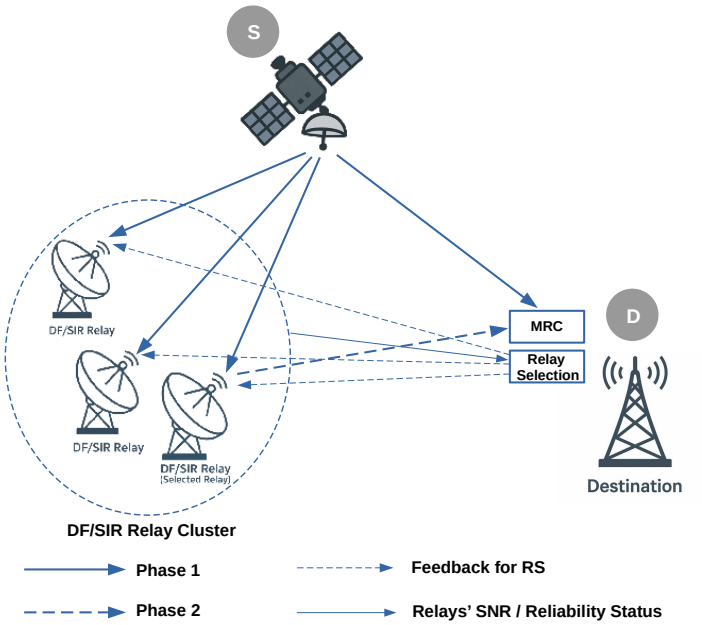


Fig. 1 HDFSIR forwarding scheme in HSTCN with relay selection.

- Monte Carlo simulation results validate the analytical derivations and demonstrate that the proposed HDFSIR protocol consistently outperforms conventional DF-only and SIR-only relaying schemes, while maintaining cooperative diversity and reducing decoding complexity under realistic mixed fading conditions.

The remainder of this paper is organized as follows. Section II describes the system model and channel assumptions for the considered hybrid satellite–terrestrial cooperative network. Section III presents the proposed HDFSIR relaying strategy, introduces the statistical modeling of the relay soft symbols, and derives the corresponding end-to-end SNR expressions. Section IV provides the analytical derivations of the outage probability and SER. Section V reports numerical and Monte Carlo simulation results, highlighting key performance trends and complexity–performance trade-offs. Finally, Section VI concludes the paper and outlines potential extensions of the proposed HDFSIR framework toward future 6G non-terrestrial network applications.

2 System Model

We consider a HSTCN composed of a single satellite source S, a set of N_R terrestrial relays $\{R_1, R_2, \ldots, R_{N_R}\}$, and a destination node D (See the network model in Fig. 1). The source information sequence is denoted by $\mathbf{u} = (u_1, \ldots, u_K)$, where K is the length of the information word. A binary channel code C_S with rate $R_S = K/N_c$ is employed at the source, where N_c denotes the codeword length. The resulting codeword $\mathbf{c} = (c_1, \ldots, c_{N_c})$ is then mapped to a modulated sequence $\mathbf{x} = (x_1, \ldots, x_{N_s})$, normalized such that $\mathbb{E}[|x_t|^2] = 1$.

The direct link between the satellite and the destination is assumed to exist but may experience severe shadowing. Communication occurs over two orthogonal phases. In the first phase, the satellite broadcasts the modulated sequence $\mathbf{x}$ to all terrestrial relays and to the destination node. The received signals at relay R_r and at the destination D are, respectively,

$$\mathbf{y}_{SR_r} = \sqrt{P_S G_{SR_r}}\, h_{SR_r}\, \mathbf{x} + \mathbf{n}_{SR_r}, \tag{1}$$

$$\mathbf{y}_{SD} = \sqrt{P_S G_{SD}}\, h_{SD}\, \mathbf{x} + \mathbf{n}_{SD}, \tag{2}$$

where P_S is the satellite transmit power, G_{SR_r} and G_{SD} denote the large-scale path-loss components corresponding to the satellite-relay and satellite-destination links, respectively, and $\mathbf{n}_{SR_r}$ and $\mathbf{n}_{SD}$ are additive white Gaussian noise (AWGN) vectors with independent entries distributed as $n_{SR_r,t}$, $n_{SD,t} \sim \mathcal{CN}(0, \sigma_n^2)$, i.e., zero-mean circularly symmetric complex Gaussian noise with variance σ_n^2. For simplicity, the same noise variance σ_n^2 is assumed on all receiving nodes. Extensions to unequal noise variances are straightforward. The fading coefficients h_{SR_r} and h_{SD} are modeled as independent Rician random variables with Rician K-factor and unit average power, $\mathbb{E}[|h|^2] = 1$. The instantaneous received SNR on the satellite-relay link is then

$$\gamma_{SR_r} = \frac{P_S G_{SR_r} |h_{SR_r}|^2}{\sigma_n^2}, \tag{3}$$

with average SNR $\overline{\gamma}_{SR_r} = \mathbb{E}[\gamma_{SR_r}] = P_S G_{SR_r}/\sigma_n^2$. The corresponding probability density function (PDF) of γ_{SR_r} under Rician fading with factor K_{SR} is given by

$$f_{\gamma_{SR_r}}(\gamma) = \frac{1 + K_{SR}}{\overline{\gamma}_{SR_r}} \exp\!\left(-K_{SR} - \frac{(1 + K_{SR})\gamma}{\overline{\gamma}_{SR_r}} \right) I_0\!\left(2\sqrt{\frac{K_{SR}(1 + K_{SR})\gamma}{\overline{\gamma}_{SR_r}}} \right), \tag{4}$$

where $I_0(\cdot)$ denotes the modified Bessel function of the first kind and order zero. An analogous expression holds for the S-D SNR γ_{SD} with its own Rician parameters $(K_{SD}, \overline{\gamma}_{SD})$.

In the second phase, all relays that successfully decode the received codeword operate in the DF mode, whereas frames that cannot be decoded with sufficient reliability are forwarded via SIR. In the SIR mode, the relay does not forward hard-decision bits. Instead, it transmits soft reliability information proportional to the LLRs of the decoded symbols. This approach mitigates error propagation while preserving power efficiency.

In the proposed HDFSIR scheme, a relay selection (RS) is performed centrally at the destination, which evaluates the instantaneous end-to-end quality of each relay by combining the satellite-relay and relay-destination link metrics under the corresponding DF or SIR mode. The destination then feeds back the index of the best relay to activate in Phase 2, ensuring that only the relay offering the highest effective reliability participates in forwarding. For analytical tractability, we assume that every relay R_r is available for consideration during the relay-selection stage.

The relay-destination link is characterized by the relay transmit power P_{R_r}, the large-scale path-loss term G_{R_rD}, and the small-scale fading coefficient h_{R_rD}. The additive noise at the destination is modeled as complex AWGN with variance σ_n^2. The instantaneous channel power gain is defined as

$$g_{R_rD} = |h_{R_rD}|^2. \tag{5}$$

The relay-destination channels are modeled as independent but not identically distributed *Nakagami-m* fading links. The PDF of the instantaneous SNR γ_{R_rD} is given by

$$f_{\gamma_{R_rD}}(\gamma) = \frac{m_r^{m_r}}{\Gamma(m_r)\,\overline{\gamma}_{R_rD}^{m_r}} \gamma^{m_r-1} \exp\left(-\frac{m_r\gamma}{\overline{\gamma}_{R_rD}}\right),$$

where $m_r \geq 0.5$ is the Nakagami fading parameter that characterizes the fading severity,

$$\overline{\gamma}_{R_rD} = \frac{P_{R_r} G_{R_rD}}{\sigma_n^2} \tag{6}$$

denotes the average SNR of the relay-destination link, and $\Gamma(\cdot)$ denotes the Gamma function.

Classical DF relaying suffers from either link exclusion when decoding fails or from error propagation when incorrect hard decisions are forwarded. The HDFSIR approach offers greater flexibility by allowing each relay to switch between DF and SIR depending on the decoding outcome, thereby mitigating error propagation in unreliable links. In the following sections, we present the proposed low-complexity HDFSIR relaying strategy and analyze its performance in HSTCNs.

3 Low-Complexity HDFSIR Strategy

In DF mode, each relay operates as in a conventional cooperative system: it performs soft-input channel decoding and forwards a reconstructed codeword whenever decoding reliability is sufficiently high. When reliable decoding cannot be guaranteed, the relay switches to SIR mode and forwards a properly normalized sequence of soft symbols derived from the Max-Log-MAP decoder output. The DF-SIR switching decision relies on external reliability indicators-most notably cyclic redundancy check (CRC) code validation-which detect residual errors after channel decoding. Because CRC-based error detection is already embedded in modern LDPC and turbo coding frameworks (e.g., DVB-S2X, 5G NTN), the switching mechanism incurs negligible overhead and requires no additional hardware. Consequently, the HDFSIR strategy can be integrated into HSTCNs with minimal architectural modifications.

In the remainder of this section, we develop a low-complexity HDFSIR scheme that offers a trade-off between decoding performance and computational efficiency. To facilitate the analytical development, the following notation is introduced and will be employed in all subsequent derivations and performance analyses.

- $y_{SR_r,t}$: received symbol at the relay R_r, $t = 1, \ldots, N_s$, where N_s is the block length.
- $\hat{h}_{SR_r}$: complex channel estimate ($S - R_r$ link).
- $\hat{\sigma}_n^2$: noise variance estimate.

- γ_{R_r}: the SNR at the output of SIR relay.
- $\mathcal{S}_M$: square M-QAM constellation, with I/Q separability.
- $\mathrm{LLR}_t^{(k)}$: de-mapper bit-LLR for bit k of the t-th symbol ($k = 1, \ldots, \log_2 M$).
- $\bar{L} = \frac{1}{N_s \log_2 M} \sum_{t,k} \left|\mathrm{LLR}_t^{(k)}\right|$: average reliability metric.
- $\tau_L^{\mathrm{DF}} > \tau_L^{\mathrm{SIR}}$: two reliability thresholds.
- $N_{\mathrm{iter}} \in \{0, 1, 2\}$: maximum SISO iterations for truncated SIR mode (0 means de-mapper only).
- $\hat{x}_{R_r,t}$: t-th soft symbol estimate at the SIR relay R_r.
- $\tilde{x}_{R_r,t} = \beta_{R_r} \hat{x}_{R_r,t}$: normalized soft symbol.
- β_{R_r}: block-wise power normalization at the relay R_r.
- $\hat{K}_{R_r}$: Rician factor estimated from block SNRs at the output of the SIR relay for statistical modeling/analysis.

The subsections below present a step-by-step, low-complexity procedure for implementing the HDFSIR relaying strategy in HSTCNs with BPSK and M-QAM modulations.

3.1 Systematic Low-Complexity HDFSIR Strategy with BPSK

For BPSK, the relay LLRs are directly proportional to the soft symbols forwarded in SIR mode. When decoding reliability is insufficient, the relay switches from DF mode to SIR mode. A low-complexity Max-Log-MAP SISO decoder [22] produces a-posteriori LLRs $L(\hat{c}_{R_r,t} \mid \mathbf{y}_{R_r})$ for $1 \leq t \leq N_c$. Fig. 2 illustrates a representative empirical distribution of the LLRs at the output of the SISO decoder for $E_b/N_0 = 10$dB. To assess the distribution of the observed LLRs, we first test the Gaussian hypothesis using the Shapiro-Wilk normality test [23]. The resulting p-value was $p_{\mathrm{Gaussian}} = 5.2 \times 10^{-5}$, which is far below the conventional significance level of 0.05. Therefore, the Gaussian model is rejected for the considered LLRs. Subsequently, we fitted a Rician distribution by maximum likelihood and evaluated the adequacy of the statistical fit using a Kolmogorov-Smirnov test [24]. In this case, the p-value was $p_{\mathrm{Rician}} = 0.13$, so the Rician hypothesis cannot be rejected. Taken together, these results indicate that the empirical distribution is significantly different from a Gaussian, while being statistically consistent with a Rician model.

To statistically characterize the soft symbols produced by the SISO decoder, we adopt a Rician-Gaussian LLR (RiGL) model. The soft symbols, derived from the a-posteriori LLRs, are modeled as follows:

$$\hat{x}_{R_r,t} = L(\hat{c}_{R_r,t} \mid \mathbf{y}_{SR_r}) = \frac{2h_{R_r}}{\sigma^2_{n_{R_r}}} \big(h_{R_r} x_t + n_{R_r,t}\big), \tag{7}$$

with $x_t \in \{-1, +1\}$ represents the transmitted BPSK modulated symbol, h_{R_r} is assumed to be a quasi-static Rician-distributed fading coefficient, and $n_{R_r,t}$ is a Gaussian noise with zero mean and variance $\sigma^2_{n_{R_r}}$.

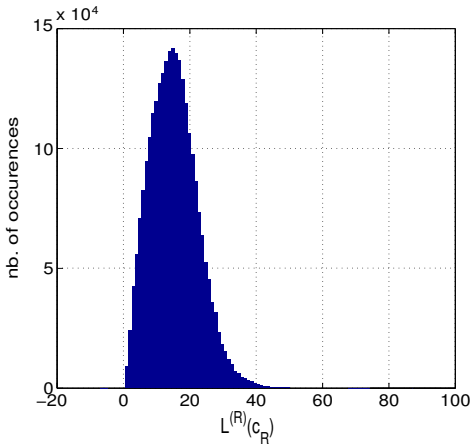


Fig. 2 Histogram of the LLRs at the output of the SISO decoder LLRs for $E_b/N_0 = 10$dB.

The relay estimates its internal SNR using the empirical second moment of the soft symbol sequence.

$$E_2 = \frac{1}{N_s} \sum_{t=1}^{N_s} \hat{x}_{R_r,t}^2,$$

The SISO-output SNR denoted by γ_{R_r} equal to $h_{R_r}^2/\sigma_{n_{R_r}}^2$ is approximated by

$$\gamma_{R_r} = \sqrt{\frac{E_2}{4} + \frac{1}{4}} - \frac{1}{2}. \tag{8}$$

Each block of soft estimated symbols is normalized by a normalization factor which is calculated by

$$\beta_{R_r} = \frac{1}{\sqrt{E\{\hat{x}_{R_r}^2\}}} = \frac{1}{\sqrt{4\gamma_{R_r}^2 + 4\gamma_{R_r}}}. \tag{9}$$

Algorithm for low-Complexity HDFSIR strategy with BPSK:

The algorithm for the low-complexity HDFSIR strategy with BPSK is summarized in the following steps:

1. **Front-end estimation:** Estimate $\hat{h}_{SR_r}$ and $\hat{\sigma}_n^2$ from pilots.
2. **Pre-LLR (Max-Log):** For each $y_{SR_r,t}$ compute $L_t = \frac{2\hat{h}_{SR_r}}{\hat{\sigma}_n^2} y_{SR_r,t}$.
3. **Reliability metric:** $\bar{L} = \frac{1}{N_s} \sum_{t=1}^{N_s} |L_t|$.
4. **Mode selection:**
   - If $\bar{L} \geq \tau_L^{\mathrm{DF}}$: attempt DF; if CRC passes, forward a clean codeword; else go to SIR with truncated SISO.
   - If $\tau_L^{\mathrm{SIR}} \leq \bar{L} < \tau_L^{\mathrm{DF}}$: SIR with truncated SISO, $N_{\mathbf{iter}} \neq 0$.
   - If $\bar{L} < \tau_L^{\mathrm{SIR}}$: De-mapper-only (SIR with truncated SISO, $N_{\mathbf{iter}} = 0$).

5. **SIR with truncated SISO:** Up to $N_{\mathbf{iter}}$ iterations to refine LLRs; use (7); compute E_2, then γ_{R_r} via (8); normalize $\tilde{x}_{R_r,t} = \beta_{R_r}\hat{x}_{R_r,t}$; transmit $\{\tilde{x}_{R_r,t}\}$ over the Nakagami-m h_{R_rD} link; optionally update $\hat{K}_{R_r}$.

The central idea of the proposed low-complexity HDFSIR mechanism is to avoid full decoding whenever the relay's decoding reliability is insufficient and to forward normalized soft symbols instead. The approach relies primarily on standard receiver front-end components (channel estimation, de-mapping) and, when needed, performs only a limited number of SISO decoding iterations (truncated decoding), thereby reducing computational overhead while maintaining robustness against decoding errors. In classical DF relaying, unsuccessful decoding at a relay typically leads either to complete link exclusion or to significant error propagation if incorrect hard decisions are forwarded. In contrast, when decoding reliability is insufficient, the proposed SIR mechanism avoids re-encoding and forwards normalized soft symbols derived from the decoder LLRs. This eliminates the need for multiple decoding iterations or symbol-mapping procedures normally required in DF-only systems. As a result, the HDFSIR approach substantially reduces the per-block computational load under unfavorable channel conditions.

3.2 Extension of the HDFSIR Strategy to M-QAM

In this section, we extend the HDFSIR strategy with BPSK to Gray coded square M-QAM by replacing the one-dimensional LLRs with bitwise LLR vectors of size $m = \log_2(M)$ and constructing complex soft symbols in SIR mode. All outer processing blocks (front-end estimation, reliability metric, switching thresholds τ_L^{DF} and τ_L^{SIR}, and block normalization) remain similar to the BPSK case.

To obtain the bitwise reliability information used in mode selection, each received symbol $y_{SR_r,t}$ is first soft de-mapped. For every bit position $k \in \{1,\ldots,m\}$, the Max-Log de-mapper computes

$$\mathrm{LLR}_t^{(k)} \approx \frac{1}{\hat{\sigma}_n^2}\left(\min_{s\in\mathcal{S}_{M,k}^{(0)}} \left|y_{SR_r,t} - \hat{h}_{SR_r}s\right|^2 - \min_{s\in\mathcal{S}_{M,k}^{(1)}} \left|y_{SR_r,t} - \hat{h}_{SR_r}s\right|^2\right), \tag{10}$$

where $\mathcal{S}_{M,k}^{(0)}$ and $\mathcal{S}_{M,k}^{(1)}$ denote the Gray-coded subsets of the M-QAM constellation whose k-th bit is equal to 0 and 1, respectively. The reliability metric is

$$\bar{L} = \frac{1}{N_s \times m}\sum_{t=1}^{N_s}\sum_{k=1}^{m}|\mathrm{LLR}_t^{(k)}|. \tag{11}$$

Soft-symbol construction:

We construct the soft symbols forwarded in SIR mode using the Normalized LLRs Soft Estimated Symbol (NL-SES) method, recently proposed in [25], which we adopt as the default estimator for M-QAM. Unlike the minimum mean-squared error (MMSE) a-posteriori probability (APP) estimator used in several classical works on soft symbol estimation [26–28], NL-SES does not average over all M constellation points. Instead,

it exploits the decomposition of square M-QAM into two $\sqrt{M}$-PAM components and constructs a nonlinear soft symbol directly from normalized bit reliabilities.

Specifically, the m LLRs of each symbol are reordered so that the first $m/2$ bits correspond to the in-phase (I) PAM component and the remaining $m/2$ bits correspond to the quadrature (Q) component under Gray labeling. The per-symbol normalized LLRs are then defined as

$$\overline{L}_t^{(k)} = \frac{\mathrm{LLR}_t^{(k)}}{\sqrt{\frac{1}{m}\sum_{i=1}^{m}\left(\mathrm{LLR}_t^{(i)}\right)^2}}, \qquad k = 1, \ldots, m.$$

Let $d = \sqrt{3/(2(M-1))}$ denote the half-step of the normalized M-QAM lattice. The corresponding I- and Q-component recursions are constructed as

$$\begin{aligned} \mathrm{I}(\hat{x}_{R_r,t}) = \overline{L}_t^{(1)}\, 2^{\frac{m}{2}-1} d + \mathrm{sign}\left(\overline{L}_t^{(1)}\right) \overline{L}_t^{(2)}\, 2^{\frac{m}{2}-2} d + \cdots \\ + \left(\prod_{k=1}^{\frac{m}{2}-1} \mathrm{sign}\left(\overline{L}_t^{(k)}\right) \right) \overline{L}_t^{(\frac{m}{2})} d, \end{aligned} \tag{12}$$

$$\begin{aligned} \mathrm{Q}(\hat{x}_{R_r,t}) = \overline{L}_t^{(\frac{m}{2}+1)}\, 2^{\frac{m}{2}-1} d + \mathrm{sign}\left(\overline{L}_t^{(\frac{m}{2}+1)}\right) \overline{L}_t^{(\frac{m}{2}+2)}\, 2^{\frac{m}{2}-2} d + \cdots \\ + \left(\prod_{k=\frac{m}{2}+1}^{m-1} \mathrm{sign}\left(\overline{L}_t^{(k)}\right) \right) \overline{L}_t^{(m)} d. \end{aligned} \tag{13}$$

and the complex soft symbol is finally obtained as

$$\hat{x}_{R_r,t} = \mathrm{I}(\hat{x}_{R_r,t}) + j\, \mathrm{Q}(\hat{x}_{R_r,t}). \tag{14}$$

This nonlinear mapping preserves the hierarchical Gray structure and scales with complexity $O(m)$ (i.e., it does not require summation over all M constellation points). It also reduces exactly to the BPSK soft symbol when $M = 2$, ensuring consistency with the binary case.

Apart from its computational advantage, NL-SES also avoids well-known limitations of APP-based averaging in the DF-SIR context. Although the APP estimator is MMSE-optimal under statistically consistent LLRs and ideal AWGN assumptions, it requires $O(M)$ operations per symbol, since it averages over all constellation points. Under unreliable or inconsistent LLRs, precisely the operating condition of SIR relaying, this averaging causes a collapse of the soft-symbol amplitude toward the constellation centroid. Such attenuation effects have been documented in several studies: Valenti and Sun [29] showed that the posterior-mean soft symbol collapses when LLRs weaken. Guillen i Fabregas *et al.* [30] demonstrated similar flattening in BICM de-mapping, and Lin *et al.* [31] reported related behavior in SIR systems.

By contrast, NL-SES operates on Gray-decomposed PAM layers with normalized reliabilities, preventing amplitude shrinkage, compensating for uneven bit reliabilities across the I/Q branches, and maintaining stable symbol geometry. As shown in [25],

this nonlinear symbol estimator yields several dB gains over classical averaging-based soft-symbol estimators for QPSK and 16-QAM in SIR relaying. In the present work, we employ the same estimator within a HDFSIR framework and, in the following paragraph, embed it into a Rician-Gaussian (RiG) model tailored to the considered HSTCN scenario.

Rician-Gaussian model and moment parameters (complex case):

The forwarded complex soft symbols obtained through the NL-SES mapping method are modeled by the RiG model given by:

$$\hat{x}_{R_r,t} = h_{R_r}\, x_t + n_{R_r,t},$$

where h_{R_r} is a Rician distributed flat fading coefficient, x_t is the transmitted M-QAM symbol and $n_{R_r,t}$ is a symmetric zero-mean complex Gaussian noise with variance $\sigma^2_{n_{R_r}}/2$ for each component. $(h_{R_r}, \sigma^2_{n_{R_r}})$ are extracted from block moments of $\hat{x}_{R_r,t}$. Let

$$E_2 = \frac{1}{N_s}\sum_{t=1}^{N_s} |\hat{x}_{R_r,t}|^2, \qquad E_4 = \frac{1}{N_s}\sum_{t=1}^{N_s} |\hat{x}_{R_r,t}|^4.$$

Using the moment method, the expressions of $h^2_{R_r}$, $\sigma^2_{n_{R_r}}$ and ultimately the SNR at the output of the SIR relay are respectively given by

$$\begin{aligned} h^2_{R_r} &= \begin{cases} \dfrac{E_2}{2} + \dfrac{\sqrt{3E_2^2 - E_4}}{2}, & E_2^2 \geq \dfrac{E_4}{3}, \\ 1, & \text{otherwise}, \end{cases} \\ \sigma^2_{n_{R_r}} &= E_2 - h^2_{R_r}, \\ \gamma_{R_r} &= \frac{h^2_{R_r}}{\sigma^2_{n_{R_r}}}. \end{aligned} \tag{15}$$

Hence, the block normalization factor is expressed as

$$\beta_{R_r} = \frac{1}{\sqrt{E\{|\hat{x}_{R_r}|^2\}}} = \frac{1}{\sqrt{h^2_{R_r} + \sigma^2_{n_{R_r}}}}. \tag{16}$$

Extension of the low-Complexity HDFSIR algorithm to M-QAM:

We follow the same processing steps as in the BPSK version and apply the same mode-selection logic and threshold values. The low-complexity HDFSIR algorithm adapted to M-QAM is presented as follows:

1. **Front-end estimation:** Estimate $\hat{h}_{SR_r}$ and $\hat{\sigma}^2_n$ from pilots.
2. **Pre-LLR (Max-Log):** Compute the Pre-LLRs via (10).
3. **Reliability metric:** Compute the reliability metric $\bar{L}$ via (11).
4. **Mode selection:**

- If $\bar{L} \geq \tau_L^{\mathrm{DF}}$: attempt DF; if CRC passes, forward a clean codeword; else go to SIR with truncated SISO.
- If $\tau_L^{\mathrm{SIR}} \leq \bar{L} < \tau_L^{\mathrm{DF}}$: SIR with truncated SISO, $N_{\mathbf{iter}} \neq 0$.
- If $\bar{L} < \tau_L^{\mathrm{SIR}}$: De-mapper-only (SIR with truncated SISO, $N_{\mathbf{iter}} = 0$).

5. **SIR with truncated SISO:** Up to $N_{\mathbf{iter}}$ iterations to refine LLRs; Using the m bit LLRs of each symbol, build $\hat{x}_{R_r,t}$ via the normalized layer-wise NL-SES mapping (I/Q PAM recursion) (12), (13) and (14) and apply the block normalization β_{R_r} via (16) to obtain $\widetilde{x}_{R_r,t} = \beta_{R_r}\hat{x}_{R_r,t}$; compute γ_{R_r}; transmit $\tilde{x}_{R_r,t}$ over the Nakagami-m h_{R_rD} link; optionally update $\hat{K}_{R_r}$.

3.3 Equivalent end-to-end SNR in SIR mode (Rician S-R / Nakagami-m R-D)

During phase 2, relay R_r transmits the normalized symbols $\tilde{x}_{R_r,t}$ with power P_{R_r} over a fading channel h_{R_rD} modeled as Nakagami-m. The t-th received symbol at the destination is expressed as

$$\begin{aligned} y_{R_rD,t} &= \sqrt{P_{R_r} G_{R_rD}}\, h_{R_rD}\, \beta_{R_r}\, \hat{x}_{R_r,t} + n_{R_rD,t}, \\ n_{R_rD,t} &\sim \mathcal{CN}\big(0, \sigma_n^2\big)\,. \end{aligned} \tag{17}$$

It is straightforward to show that the equivalent end-to-end SNR in SIR mode with BPSK and M-QAM modulations can be expressed by

$$\gamma_{SR_rD} = \frac{\bar{\gamma}_{R_rD}\, g_{R_rD}\, \gamma_{R_r}}{\bar{\gamma}_{R_rD}\, g_{R_rD} \;+\; \gamma_{R_r} \;+\; 1}, \tag{18}$$

where g_{R_rD} is the instantaneous power gain defined in (5), $\bar{\gamma}_{R_rD}$ is the average SNR of the relay-destination link given in (6), and γ_{R_r} denotes the SNR at the output of the SISO decoder as previously defined. The statistical properties relevant to the SNR expression are as follows:

- The relay-destination fading power gain g_{R_rD} is Gamma-distributed.
- γ_{R_r} is the relay's per-block SISO output SNR. Since the complex channel gain h_{R_r} follows a Rician fading model, the SNR $\gamma_{R_r} = |h_{R_r}|^2/\sigma^2_{n_{R_r}}$ exhibits Rician power statistics with a corresponding factor, whose estimate $\hat{K}_{R_r}$ will be derived in subsection 3.5.

3.4 Destination-Side Combining

Once all relays have determined their operating mode (DF or SIR), each relay R_r computes an effective end-to-end SNR (DF or SIR) denoted by γ_{SR_rD}. In SIR mode, this SNR is given by the expression in (18), while in DF mode the standard bottleneck

rule $\min(\gamma_{R_r}, \gamma_{R_r D})$ applies, i.e.,

$$\begin{aligned}
\gamma_{SR_rD} &= \begin{cases} \gamma_r^{\mathrm{SIR}}, & \text{if } R_r \text{ operates in SIR mode,} \\ \gamma_r^{\mathrm{DF}}, & \text{if } R_r \text{ decodes correctly,} \end{cases} \\
\gamma_r^{\mathrm{SIR}} &= \frac{\bar{\gamma}_{R_rD}\, g_{R_rD}\, \gamma_{R_r}}{\bar{\gamma}_{R_rD}\, g_{R_rD} + \gamma_{R_r} + 1}, \\
\gamma_r^{\mathrm{DF}} &= \min(\gamma_{R_r}, \gamma_{R_rD})\,.
\end{aligned} \tag{19}$$

Relay selection: Before the transmitted signal arrives at the destination node, the cooperative subsystem performs opportunistic relay selection: among the N_R relays, only the relay providing the highest instantaneous end-to-end SNR is selected, i.e.,

$$\gamma_{\mathrm{SRD,sel}} = \max_{1 \le r \le N_R} \gamma_{SR_rD}. \tag{20}$$

The best selected relays is determined at the destination nodes that inform the relays to transmit or keep idle through a feedback channel. This selection step allows the receiver to exploit full diversity through both DF and SIR relays, regardless of each relay's decoding outcome.

MRC at the destination: The destination receives two statistically independent contributions: (i) the direct satellite-destination signal, with instantaneous SNR γ_{SD}, and (ii) the relayed signal from the selected relay, with SNR $\gamma_{\mathrm{SRD,sel}}$. Since noise terms across the two paths are independent, maximal-ratio combining (MRC) yields the total received SNR

$$\gamma_{\mathrm{eq}} = \gamma_{SD} + \gamma_{\mathrm{SRD,sel}}. \tag{21}$$

Since the selected relay may operate in either DF or SIR mode, the random variable $\gamma_{\mathrm{SRD,sel}}$ is distributed as the maximum of a mixture of Rician-Nakagami DF paths and Rician-Nakagami SIR paths. Importantly, the SIR branch inherits the Rician statistics of the satellite-relay link through the SISO-output SNR γ_{R_r}, while the second hop contributes Nakagami-m fading through h_{R_rD}. Thus, the equivalent end-to-end channel of the selected cooperative path is a mixture of Rician-Gamma distributed components, providing a tractable structure for the outage and SER analyses developed in the next section.

3.5 Rician-K extraction for the SIR-relay output SNR

The SIR relay produces block-wise soft symbols from the SISO decoder output and normalizes them by β_{R_r}, then forwards them over the $R-D$ link. The SISO block-b output SNR $\hat{\gamma}_{R_r}^{(b)}$ is estimated via (8) for BPSK and via (15) for M-QAM. Over many blocks, the sequence $\{\hat{\gamma}_{R_r}^{(b)}\}_{b=1}^{B}$ captures the slow variations of the effective $S - R_r$ channel that remain in the soft decisions after decoding.

Key modeling link:

Under the assumption that the per-block SISO output SNR γ_{R_r} follows a Rician power distribution characterized by the relay-dependent factor K_{R_r}, its statistics correspond to a non-central χ^2 random variable with two degrees of freedom. Based on this model, the estimated factor $\hat{K}_{R_r}$ is obtained from the corresponding scale-free moment ratio

$$\rho_{R_r} \triangleq \frac{\mathrm{Var}[\gamma_{R_r}]}{(\mathbb{E}[\gamma_{R_r}])^2}, \tag{22}$$

which depends only on the Rician factor K_{R_r}, as derived in [32]:

$$\rho_{R_r} = \frac{1 + 2K_{R_r}}{(1 + K_{R_r})^2}. \tag{23}$$

Closed-form, one-pass MoM estimator:

The sample mean and variance of the block SNRs is computed by

$$\bar{\gamma}_{R_r} = \frac{1}{B}\sum_{b=1}^{B} \gamma_{R_r}^{(b)}, \qquad s^2_{\gamma_{R_r}} = \frac{1}{B-1}\sum_{b=1}^{B} \left(\gamma_{R_r}^{(b)} - \bar{\gamma}_{R_r}\right)^2,$$

and form the empirical, scale-free ratio $\hat{\rho}_{R_r} = s^2_{\gamma_{R_r}}/\bar{\gamma}^2_{R_r}$. Inverting (23) yields the closed-form estimate

$$\hat{K}_{R_r} = \frac{(1 - \hat{\rho}_{R_r}) + \sqrt{1 - \hat{\rho}_{R_r}}}{\hat{\rho}_{R_r}}, \qquad 0 < \hat{\rho}_{R_r} < 1\,. \tag{24}$$

We substitute the estimated Rician factor $\hat{K}_{R_r}$ into the Rician PDF/CDF expressions governing the SIR-relay output SNR, which are subsequently employed in the outage and SER analyses presented in the next section. Since the estimator relies solely on the block-wise soft-symbol moments, it operates entirely online and requires no additional pilots, training sequences, or signaling overhead

4 Outage Probability of Opportunistic HDFSIR Relaying in HSTCN

This section develops the outage probability analysis of the opportunistic HDFSIR scheme operating in HSTCN.

4.1 DF Success Probability and Threshold Design

Let γ_{dec} denote the decoding-reliability threshold at the relay, expressed in terms of the SISO output SNR γ_{R_r}. Each relay R_r attempts DF if $\gamma_{R_r} \geq \gamma_{\mathrm{dec}}$, otherwise it operates in SIR mode. Hence, we define the DF success probability by the expression

$$p_r \triangleq \Pr\{\gamma_{R_r} \geq \gamma_{\mathrm{dec}}\} = 1 - F_{\gamma_{R_r}}(\gamma_{\mathrm{dec}}), \tag{25}$$

where $F_{\gamma_{R_r}}(\cdot)$ is the CDF of the Rician-SNR γ_{R_r}. The Rician-SNR CDF can be written in terms of the Marcum-Q function $Q_1(\cdot,\cdot)$ as

$$F_{\gamma_{R_r}}(x) = 1 - Q_1\left(\sqrt{2K_{R_r}}, \sqrt{\frac{2(1+K_{R_r})}{\bar{\gamma}_{R_r}}\, x}\right), \quad x \geq 0, \tag{26}$$

so that (25) yields

$$p_r = Q_1\left(\sqrt{2K_{R_r}}, \sqrt{\frac{2(1+K_{R_r})}{\bar{\gamma}_{R}}\, \gamma_{\mathrm{dec}}}\right). \tag{27}$$

In practice, the decoding threshold γ_{dec} is implemented through a decision rule on the average LLR magnitude $\bar{L}$, as described in Section 3.1 for BPSK and Section 3.2 for M-QAM. The mapping $\bar{L} \mapsto \gamma_{\mathrm{dec}}$ is obtained off-line by calibrating the relay's demapper/decoder output against the first-hop S-R SNR. More precisely, γ_{dec} is chosen as the SNR at which the channel decoder meets a prescribed frame-error-rate (FER) target, such that DF is enabled only in operating regions where error propagation is negligible. Typical design points are

$$\mathrm{FER}_{\mathrm{decoder}}(\gamma_{\mathrm{dec}}) \approx 10^{-3} \text{ or } 10^{-4},$$

depending on the adopted coded modulation scheme and the required reliability of the cooperative link.

4.2 Per-Relay End-to-End SNR CDFs

Let X_r denote the end-to-end SNR contributed by relay R_r:

$$X_r = \begin{cases} \gamma_r^{\mathrm{DF}}, & \text{if } \gamma_{R_r} \geq \gamma_{\mathrm{dec}} \quad \text{(DF mode)}, \\ \gamma_r^{\mathrm{SIR}}, & \text{if } \gamma_{R_r} < \gamma_{\mathrm{dec}} \quad \text{(SIR mode)}. \end{cases} \tag{28}$$

Conditioning on the DF-SIR decision, the marginal CDF of X_r can be written as

$$F_{X_r}(x) = p_r\, F_{\gamma_r^{\mathrm{DF}}}(x \mid \gamma_{R_r} \geq \gamma_{\mathrm{dec}}) + (1-p_r)\, F_{\gamma_r^{\mathrm{SIR}}}(x \mid \gamma_{R_r} < \gamma_{\mathrm{dec}}). \tag{29}$$

For analytical tractability, the conditional CDFs are replaced by their unconditional forms. This yields an accurate yet closed-form mixture representation:

$$F_{X_r}(x) \;\approx\; p_r\, F_{\gamma_r^{\mathrm{DF}}}(x) + (1-p_r)\, F_{\gamma_r^{\mathrm{SIR}}}(x), \tag{30}$$

an approximation which is accurate because the DF-SIR switching decision is itself governed by γ_{R_r}, and the end-to-end SNR expressions exhibit the same dominant exponential tail behavior regardless of the conditioning.

Assuming independence between the first and second hops, we have

$$\begin{aligned} F_{\gamma_r^{\mathrm{DF}}}(x) &= \Pr\big(\min(\gamma_{R_r}, \gamma_{R_rD}) \le x\big) \\ &= 1 - \big(1 - F_{\gamma_{R_r}}(x)\big)\big(1 - F_{\gamma_{R_rD}}(x)\big). \end{aligned} \tag{31}$$

where $F_{\gamma_{R_r}}(x)$ is the Rician-SNR CDF as defined in (26) and $F_{\gamma_{R_rD}}(x)$ is the Nakagami-m_r CDF for the relay-destination link SNR. Writing $\gamma_{R_rD} = \bar{\gamma}_{R_rD} g_{R_rD}$ with $g_{R_rD} \sim \mathrm{Gamma}(m_r, \theta_r)$ and $\theta_r = \Omega_r/m_r$, we obtain

$$F_{\gamma_{R_rD}}(x) = \frac{\gamma\big(m_r,\, x/(\bar{\gamma}_{R_rD}\theta_r)\big)}{\Gamma(m_r)}. \tag{32}$$

Condition on the event that the relay decoder outputs an instantaneous SNR of $\gamma_{R_r} = \gamma$, and fix an arbitrary threshold $x \ge 0$. Under this conditioning, from the end-to-end SIR SNR generated by relay R_r is governed by the expression in (18),

$$\gamma_r^{\mathrm{SIR}} = \frac{\bar{\gamma}_{R_rD} g_{R_rD}\, \gamma}{\bar{\gamma}_{R_rD} g_{R_rD} + \gamma + 1},$$

we observe that γ_r^{SIR} is an increasing function of g_{R_rD} for fixed γ. Thus, the event $\{\gamma_r^{\mathrm{SIR}} \le x\}$ can be inverted in closed form.
Case 1: $\gamma \le x$**:** Since the SIR expression satisfies $\gamma_r^{\mathrm{SIR}} < \gamma$, the inequality $\gamma_r^{\mathrm{SIR}} \le x$ holds automatically for all realizations of g_{R_rD}. Hence,

$$\Pr\big(\gamma_r^{\mathrm{SIR}} \le x \,\big|\, \gamma_{R_r} = \gamma\big) = 1, \qquad 0 \le \gamma \le x.$$

Case 2: $\gamma > x$**:** Solving the inequality $\gamma_r^{\mathrm{SIR}} \le x$ for g_{R_rD} yields

$$g_{R_rD} \;\le\; \frac{x(\gamma+1)}{\bar{\gamma}_{R_rD}(\gamma - x)}.$$

Thus, for $\gamma > x$ we obtain

$$\Pr\big(\gamma_r^{\mathrm{SIR}} \le x \,\big|\, \gamma_{R_r} = \gamma\big) = F_{g_{R_rD}}\left(\frac{x(\gamma+1)}{\bar{\gamma}_{R_rD}(\gamma - x)}\right),$$

where $F_{g_{R_rD}}(y) = \gamma(m_r, y/\theta_r)\,/\Gamma(m_r)$ is the Gamma CDF of the Nakagami-m_r fading amplitude squared. Averaging over the Rician-distributed SNR γ_{R_r} produces the exact unconditional CDF:

$$F_{\gamma_r^{\mathrm{SIR}}}(x) = \int_0^x f_{\gamma_{R_r}}(\gamma)\, d\gamma + \int_x^\infty F_{g_{R_rD}}\left(\frac{x(\gamma+1)}{\bar{\gamma}_{R_rD}(\gamma - x)}\right) f_{\gamma_{R_r}}(\gamma)\, d\gamma. \tag{33}$$

where $f_{\gamma_{R_r}}(\gamma)$ is the Rician-SNR pdf.

4.3 Relay Selection and MRC Outage Probability

Let X_r have CDF $F_{X_r}(x)$ as in (30). Under independent relays, the SNR of the selected relay path is

$$\gamma_{\mathrm{SRD,sel}} = \max_{1\le r\le N_R} X_r, \tag{34}$$

with CDF

$$F_{\gamma_{\mathrm{SRD,sel}}}(x) = \prod_{r=1}^{N_R} F_{X_r}(x). \tag{35}$$

At the destination, MRC combines the direct S-D branch and the selected relay path. Let γ_{SD} denote the S-D SNR, modeled as Rician with factor K_{SD} and average SNR $\bar{\gamma}_{SD}$. The equivalent SNR at the destination is

$$\gamma_{\mathrm{eq}} = \gamma_{SD} + \gamma_{\mathrm{SRD,sel}}. \tag{36}$$

The outage probability at threshold γ_{th} is thus

$$\begin{aligned} P_{\mathrm{out}}(\gamma_{\mathrm{th}}) &= \Pr\big(\gamma_{SD} + \gamma_{\mathrm{SRD,sel}} \le \gamma_{\mathrm{th}}\big) \\ &= \int_0^{\gamma_{\mathrm{th}}} F_{\gamma_{\mathrm{SRD,sel}}}(\gamma_{\mathrm{th}} - z)\, f_{\gamma_{SD}}(z)\, dz. \end{aligned} \tag{37}$$

where $f_{\gamma_{SD}}(z)$ denotes the Rician SNR pdf, given in a form analogous to the distribution in (4) but with the corresponding Rician factor K_{SD}.

4.4 Closed-Form Integrand via a Tight SIR Bound

To obtain a closed-form integrand for (37) while maintaining good accuracy, we use the inequality

$$\frac{ab}{a+b+1} \le \min(a,b), \qquad a,b \ge 0, \tag{38}$$

which implies

$$\gamma_r^{\mathrm{SIR}} \;\le\; \min\left(\gamma_{R_r},\, \bar{\gamma}_{R_rD} g_{R_rD}\right). \tag{39}$$

Accordingly, we approximate $F_{\gamma_r^{\mathrm{SIR}}}(x)$ by the CDF of the upper-bounding random variable $min(\gamma_{R_r}, \bar{\gamma}_{R_rD} g_{R_rD})$ as follows

$$F_{\gamma_r^{\mathrm{SIR}}}(x) \approx 1 - \big(1 - F_{\gamma_{R_r}}(x)\big)\big(1 - F_{\bar{\gamma}_{R_rD} g_{R_rD}}(x)\big), \tag{40}$$

where

$$F_{\bar{\gamma}_{R_rD} g_{R_rD}}(x) = \frac{\gamma\Big(m_r,\, \frac{x}{\bar{\gamma}_{R_rD}\,\theta_r}\Big)}{\Gamma(m_r)}. \tag{41}$$

This step yields a tight analytical approximation to $F_{\gamma_r^{\mathrm{SIR}}}$, hence the resulting outage expression is approximate. Using the series $I_0(2\sqrt{ux}) = \sum_{n=0}^{\infty} (ux)^n/(n!)^2$, the Rician

SNR pdf can be written as

$$f_{\gamma_{R_r}}(x) = \frac{1+K_{R_r}}{\bar{\gamma}_{R_r}} e^{-K_{R_r}} \sum_{n=0}^{\infty} \frac{1}{(n!)^2} \left(\frac{K_{R_r}(1+K_{R_r})}{\bar{\gamma}_{R_r}} \right)^n x^n \exp\left(-\frac{(1+K_{R_r})x}{\bar{\gamma}_{R_r}} \right). \tag{42}$$

Integrating (42) with respect to x, the CDF of the Rician SNR can be written as

$$F_{\gamma_{R_r}}(x) = e^{-K_{R_r}} \sum_{n=0}^{\infty} \frac{1}{(n!)^2} \left(\frac{K_{R_r}(1+K_{R_r})}{\bar{\gamma}_{R_r}} \right)^n \frac{\gamma\left(n+1, \frac{(1+K_{R_r})x}{\bar{\gamma}_{R_r}}\right)}{\left(\frac{1+K_{R_r}}{\bar{\gamma}_{R_r}}\right)^n}. \tag{43}$$

where $\gamma(\cdot,\cdot)$ denotes the lower incomplete Gamma function. For numerical evaluation, the series in (43) is truncated to $n \leq N_{\max}$, yielding a finite sum of exponential-polynomial terms.

When $m_r \in \mathbb{N}$ (which is common in practice), the Nakagami-m CDF $F_{\bar{\gamma}_{R_r D} g_{R_r D}}(x)$ admits the finite-sum form

$$F_{\bar{\gamma}_{R_r D} g_{R_r D}}(x) = 1 - \exp\left(-\frac{x}{\bar{\gamma}_{R_r D}\theta_r} \right) \sum_{k=0}^{m_r-1} \frac{1}{k!} \left(\frac{x}{\bar{\gamma}_{R_r D}\theta_r} \right)^k. \tag{44}$$

Inserting (44) and the Rician SNR distribution (kept in Marcum-Q form or represented via its standard series expansion) into (31) and (40), each per-relay CDF $F_{X_r}(x)$ can be represented as a (generally infinite, and in practice truncated) linear combination of exponential-polynomial terms of the form $x^n e^{-\beta x}$ with $\beta > 0$ [32].

Consequently, after truncation of the Rician series and expansion of the Nakagami-m finite sums, the selection CDF $F_{\gamma_{SRD,\text{sel}}}(x) = \prod_{r=1}^{N_R} F_{X_r}(x)$ can be reorganized and represented as a truncated linear combination of exponential-polynomial terms,

$$F_{\gamma_{\text{SRD,sel}}}(x) = 1 - \sum_{\ell=1}^{L^{(\text{sel})}} A_\ell^{(\text{sel})} e^{-B_\ell^{(\text{sel})} x} \sum_{i=0}^{R_\ell^{(\text{sel})}} d_{\ell,i}^{(\text{sel})} x^i, \tag{45}$$

where the coefficients $\{A_\ell^{(\text{sel})}, B_\ell^{(\text{sel})}, d_{\ell,i}^{(\text{sel})}\}$ depend on the link statistics (including p_r) and on the chosen truncation order $N_{\max}$. P_r is absorbed into coefficients. It is emphasized that (45) is obtained without assuming identically distributed relay links. In this case, the coefficients $\{A_\ell^{(\text{sel})}, B_\ell^{(\text{sel})}, d_{\ell,i}^{(\text{sel})}\}$ implicitly capture the heterogeneity of the individual relay statistics.

For clarity, we emphasize that the relay decoding success probability $p_r = \Pr(\gamma_{R_r} \geq \gamma_{\text{dec}})$, which explicitly is present in the per-relay mixture model in (30), is not neglected in the subsequent analysis. Once the DF and SIR end-to-end SNR CDFs are represented in a unified exponential-polynomial form, the weighted combination $p_r F_{\gamma_r^{\text{DF}}}(x) + (1-p_r) F_{\gamma_r^{\text{SIR}}}(x)$ can be equivalently rewritten within the same functional structure, with the factor p_r incorporated into the corresponding coefficients. After relay selection has been carried out, the product of the per-relay CDFs preserves this

structure, yielding the representation in (45), where all relay-dependent parameters, including the decoding probabilities, are implicitly embedded in the constants A_ℓ and $d_{\ell,i}$.

4.5 Closed-Form Outage Expression

Using (45) in (37), the outage probability becomes

$$P_{\text{out}}(\gamma_{\text{th}}) = \int_0^{\gamma_{\text{th}}} \left[1 - \sum_{\ell=1}^{L^{(\text{sel})}} A_\ell^{(\text{sel})} e^{-B_\ell^{(\text{sel})}(\gamma_{\text{th}}-z)} \sum_{i=0}^{R_\ell^{(\text{sel})}} d_{\ell,i}^{(\text{sel})} (\gamma_{\text{th}} - z)^i\right] f_{\gamma_{SD}}(z)\, dz. \quad (46)$$

The Rician pdf (4) with Rician factor K_{SD} admits the Bessel-series representation

$$f_{\gamma_{SD}}(z) = \frac{1+K_{SD}}{\bar{\gamma}_{SD}}\, e^{-K_{SD}} \exp\Big(-\frac{(1+K_{SD})z}{\bar{\gamma}_{SD}}\Big) \sum_{n=0}^{\infty} \frac{1}{(n!)^2} \left(\frac{K_{SD}(1+K_{SD})}{\bar{\gamma}_{SD}}\, z\right)^n. \quad (47)$$

Thus the integrand becomes a linear combination of terms of the type

$$z^n e^{-az}\, (\gamma_{\text{th}} - z)^i e^{-B_\ell^{(\text{sel})}(\gamma_{\text{th}}-z)}, \quad \text{where} \quad a = \frac{1+K_{SD}}{\bar{\gamma}_{SD}}.$$

Define the convolution integral

$$\mathcal{I}_{n,i}(a,b;\gamma_{\text{th}}) \triangleq \int_0^{\gamma_{\text{th}}} z^n\, e^{-az} (\gamma_{\text{th}} - z)^i\, e^{-b(\gamma_{\text{th}}-z)}\, dz, \quad a,b>0. \quad (48)$$

Using the change of variables $z = \gamma_{\text{th}} u$ and standard identities for the Beta function and confluent hyper-geometric functions, one obtains the following closed form:

$$\mathcal{I}_{n,i}(a,b;\gamma_{\text{th}}) = e^{-b\gamma_{\text{th}}}\, \gamma_{\text{th}}^{n+i+1} \mathrm{B}(n+1, i+1)\, {}_1F_1\big(n+1;\, n+i+2;\, (b-a)\gamma_{\text{th}}\big). \quad (49)$$

where $\mathrm{B}(\cdot,\cdot)$ is the Beta function and ${}_1F_1(\cdot;\cdot;\cdot)$ is the confluent hyper-geometric function of the first kind. Collecting all constants, the outage probability can be expressed as

$$P_{\text{out}}(\gamma_{\text{th}}) = 1 - e^{-K_{SD}} \sum_{n=0}^{\infty} \sum_{\ell=1}^{L^{(\text{sel})}} \sum_{i=0}^{R_\ell^{(\text{sel})}} C_{\ell,n,i}\, \mathcal{I}_{n,i}\big(a, B_\ell^{(\text{sel})}; \gamma_{\text{th}}\big), \quad (50)$$

with

$$\begin{aligned} a &= \frac{1+K_{SD}}{\bar{\gamma}_{SD}}, \\ C_{\ell,n,i} &= A_\ell^{(\text{sel})}\, d_{\ell,i}^{(\text{sel})} \frac{1+K_{SD}}{\bar{\gamma}_{SD}} \frac{1}{(n!)^2} \left(\frac{K_{SD}(1+K_{SD})}{\bar{\gamma}_{SD}}\right)^n. \end{aligned} \quad (51)$$

and $\mathcal{I}_{n,i}(\cdot)$ given by (49). Because L and all R_ℓ are finite for integer m, (50) is a finite sum over (ℓ, i) and an infinite but rapidly convergent sum over n. In computations, this sum is truncated at N_{max}.

5 Symbol Error Rate of Opportunistic HDFSIR in HSTCN

Recalling the equivalent SNR γ_{eq} introduced in the previous section, its MRC form can be written as $\gamma_{\text{eq}} = \gamma_{SD} + \gamma_{\text{SRD,sel}}$, where γ_{SD} denotes the Rician S-D SNR and $\gamma_{\text{SRD,sel}} = \max_{1\le r\le N_R} X_r$ represents the selected end-to-end SNR across relays, with X_r defined in (28). All links and relays are assumed independent. Building on the equivalent end-to-end SNR model introduced above, we now derive average SER expressions using the moment generating function (MGF) framework.

5.1 MGF-based SER expressions

For a coherent constellation, the average SER can be written in terms of the MGF $M_{\gamma_{\text{eq}}}(s) \triangleq \mathbb{E}\big[e^{-s\gamma_{\text{eq}}}\big]$:

$$P_s^{\text{BPSK}} = \frac{1}{\pi}\int_0^{\pi/2} M_{\gamma_{\text{eq}}}\left(\frac{1}{\sin^2\theta}\right) d\theta, \tag{52}$$

$$P_s^{M\text{-QAM}} \approx \frac{4}{\pi}\left(1-\frac{1}{\sqrt{M}}\right)\int_0^{\pi/2} M_{\gamma_{\text{eq}}}\left(\frac{3}{2(M-1)\sin^2\theta}\right) d\theta - \frac{4}{\pi}\left(1-\frac{1}{\sqrt{M}}\right)^2\int_0^{\pi/4} M_{\gamma_{\text{eq}}}\left(\frac{3}{2(M-1)\sin^2\theta}\right) d\theta. \tag{53}$$

Because γ_{SD} and $\gamma_{\text{SRD,sel}}$ are independent, the MGF of γ_{eq} is simply the product of their individual MGFs:

$$M_{\gamma_{\text{eq}}}(s) = M_{\gamma_{SD}}(s)\, M_{\gamma_{\text{SRD,sel}}}(s). \tag{54}$$

5.2 Constituent MGFs

The S-D hop follows the Rician SNR distribution $f_{\gamma_{SD}}(z)$ given in (4), with the Rician factor replaced by K_{SD}. Since the corresponding MGF does not admit a simple finite closed-form expression, it is evaluated numerically via its defining Laplace transform [32]:

$$M_{\gamma_{SD}}(s) = \int_0^{\infty} e^{-sz}\, f_{\gamma_{SD}}(z)\, dz. \tag{55}$$

For the selected relay path, the CDF satisfies $F_{\gamma_{\text{SRD,sel}}}(x) = \prod_{r=1}^{N_R} F_{X_r}(x)$, which leads to the pdf $f_{\gamma_{\text{SRD,sel}}}(x) = \sum_{r=1}^{N_R} f_{X_r}(x)\prod_{j\neq r} F_{X_j}(x)$. Consequently,

$$M_{\gamma_{\text{SRD,sel}}}(s) = \sum_{r=1}^{N_R}\int_0^{\infty} e^{-sx}\, f_{X_r}(x)\prod_{j\neq r} F_{X_j}(x)\, dx. \tag{56}$$

At this stage, no assumption of identically distributed relays is imposed. The expression in (56) holds for independent but statistically non-identical relay links. Each

F_{X_r} is the unconditional mixture $F_{X_r}(x) = p_r\, F_{\gamma_r^{\mathrm{DF}}}(x) + (1-p_r)\, F_{\gamma_i^{\mathrm{SIR}}}(x)$, where $p_r = \Pr\{\gamma_{R_i} \geq \gamma_{\mathrm{dec}}\}$ is given in (27). $F_{\gamma_r^{\mathrm{DF}}}(x)$ is given in (31), and $F_{\gamma_r^{\mathrm{SIR}}}(x)$ follows the integral form in (33). The derivative $f_{X_r}(x)$ is obtained by differentiating this mixture.

5.3 Closed-form integrand route (tight upper bound)

For efficient evaluation when m_r is an integer, we employ the tight SIR upper bound $\gamma_i^{\mathrm{SIR}} \leq \min(\gamma_{R_r}, \bar{\gamma}_{R_rD} g_{R_rD})$, which leads to the closed-form CDF in (40). As mentioned above, $F_{\bar{\gamma}_{R_rD} g_{R_rD}}(x)$ reduces to a finite polynomial multiplied by an exponential term (cf. (44)). For a tractable closed-form evaluation of the MGF, we assume i.i.d. relays sharing the same parameters (m, K_s, $\bar{\gamma}_R$, $\bar{\gamma}_{RD}$) and a common decoding threshold. The distributions simplify to $F_{X_r} \equiv F_X$ and $f_{X_r} \equiv f_X$. Under this symmetry, (56) reduces to

$$M_{\gamma_{\mathrm{SRD,sel}}}(s) = N_R \int_0^\infty e^{-sx}\, f_X(x) \left(F_X(x)\right)^{N_R-1} dx. \tag{57}$$

As previously mentioned, $F_X(x)$ can be expressed as a finite linear combination of exponential-polynomial terms in form of

$$F_X(x) = 1 - \sum_{\ell=1}^{L} A_\ell e^{-B_\ell x} \sum_{i=0}^{R_\ell} d_{\ell,i} x^i, \tag{58}$$

where $\{A_\ell, B_\ell, d_{\ell,i}\}$ are constants determined by the link statistics. Let $T(x)$ be the tail polynomial-exponential sum defined by $T(x) = 1 - F_X(x)$. Then

$$f_X(x) = \frac{d}{dx} F_X(x) = -T'(x), \tag{59}$$

and differentiating term-by-term gives the explicit finite representation

$$f_X(x) = \sum_{\ell=1}^{L} A_\ell e^{-B_\ell x} \sum_{q=0}^{R_\ell} \underbrace{\left(B_\ell d_{\ell,q} - (q+1) d_{\ell,q+1}\right)}_{\triangleq\, \tilde{d}_{\ell,q}} x^q, \tag{60}$$

with the convention $d_{\ell,R_\ell+1} = 0$.

Next, we expand $\left(F_X(x)\right)^{N_R-1} = \left(1 - T(x)\right)^{N_R-1}$ by the binomial theorem as follows:

$$\left(F_X(x)\right)^{N_R-1} = \sum_{m=0}^{N_R-1} \binom{N_R-1}{m} (-1)^m \left(T(x)\right)^m. \tag{61}$$

Since $T(x)$ is a finite sum of terms of the form $e^{-B_\ell x}x^i$, its m-th power can be expanded by multi-nomial convolution. A convenient way to write it is:

$$\big(T(x)\big)^m = \sum_{\boldsymbol{\ell}\in\{1,\dots,L\}^m} \left(\prod_{t=1}^{m} A_{\ell_t}\right) e^{-\left(\sum_{t=1}^{m} B_{\ell_t}\right)x} \sum_{k=0}^{K(\boldsymbol{\ell})} \eta_{\boldsymbol{\ell},k}\, x^k, \tag{62}$$

where $K(\boldsymbol{\ell}) = \sum_{t=1}^{m} R_{\ell_t}$ and $\eta_{\boldsymbol{\ell},k}$ is obtained by polynomial convolution of $\left(\sum_{i=0}^{R_{\ell_t}} d_{\ell_t,i}x^i\right)$ over $t = 1,\dots,m$.

Substituting (60) and (61)-(62) into (57), the integrand becomes a finite sum of terms of the form $e^{-(s+\beta)x}x^n$, whose Laplace integral is [32]

$$\int_0^\infty e^{-(s+\beta)x}x^n\,dx = \frac{n!}{(s+\beta)^{n+1}}, \qquad \Re\{s+\beta\} > 0. \tag{63}$$

Therefore, collecting coefficients yields the fully finite-sum form of the MGF function:

$$\begin{aligned} M_{\gamma_{\mathrm{SRD,sel}}}(s) = N_R \sum_{m=0}^{N_R-1} \binom{N_R-1}{m} (-1)^m \sum_{\ell_0=1}^{L} \sum_{q=0}^{R_{\ell_0}} \left(A_{\ell_0}\tilde{d}_{\ell_0,q}\right) \sum_{\boldsymbol{\ell}\in\{1,\dots,L\}^m} \left(\prod_{t=1}^{m} A_{\ell_t}\right) \\ \times \sum_{k=0}^{K(\boldsymbol{\ell})} \eta_{\boldsymbol{\ell},k} \frac{(q+k)!}{\left(s + B_{\ell_0} + \sum_{t=1}^{m} B_{\ell_t}\right)^{q+k+1}}. \end{aligned} \tag{64}$$

Consequently, $M_{\gamma_{\mathrm{SRD,sel}}}(s)$ in (56) (or (57)) reduces to a finite sum of rational functions in s, from which the overall MGF $M_{\gamma_{\mathrm{eq}}}(s)$ follows directly via (54). Substituting this expression into (52)-(53) leaves only the outer θ-integration, which is a smooth one-dimensional integral.

6 Simulation results

In this section, the performance of the proposed HDFSIR relaying scheme is assessed by Monte-Carlo simulation and compared with conventional DF-only and SIR-only relaying. Unless otherwise stated, all channels are assumed to be frequency-flat and impaired by additive white Gaussian noise. The source-to-relay (S→R) and source-to-destination (S→D) links are modeled as Rician fading channels with factor K, while the relay-to-destination (R→D) link follows a Nakagami-m distribution. Unless otherwise specified, numerical results are reported for the representative mixed-fading case with $K = 5$ on the S→R and S→D links and $m = 1$ on the R→D link.

For the outage probability results, BPSK modulation is employed and the average SNR per bit refers to the total transmitted power. The relay performs SISO decoding and CRC verification. If the CRC fails or the decoding reliability falls below the prescribed threshold γ_{dec}, the relay switches to SIR-based forwarding. In the SER analysis, different modulation formats (BPSK, QPSK, and M-QAM constellations)

are considered in order to quantify the impact of modulation order on the end-to-end detection performance. The analytical expressions derived in the paper are plotted together with the Monte-Carlo curves, allowing direct validation of the accuracy of the proposed theoretical framework.

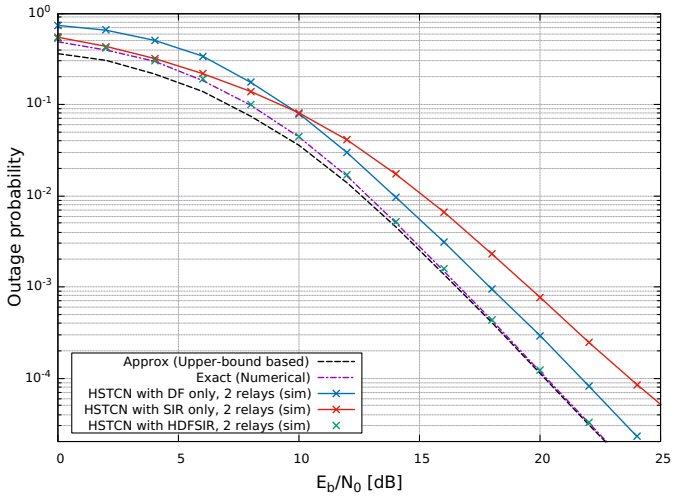


Fig. 3 Outage probability performance of the HSTCN versus E_b/N_0 for DF-only, SIR-only, and the proposed HDFSIR relaying scheme over cascaded Rician (S↛R and S↛D) and Nakagami-m (R↛D) fading channels.

Fig. 3 compares the outage probability performance of the HSTCN when deploying DF-only, SIR-only, and the proposed HDFSIR relaying scheme as a function of the average SNR per bit over cascaded Rician (S↛R and S↛D) and Nakagami-m (R↛D) fading channels. The SIR-only scheme exhibits a smooth decay of the outage probability with increasing SNR, reflecting its robustness against decoding errors at low SNR. In contrast, DF-only relaying achieves a steeper slope at high SNR due to the availability of reliable decoding and full diversity, but suffers from a higher outage probability in the low-to-mid SNR region as a consequence of decoding failures and error propagation. The proposed HDFSIR scheme adaptively combines the two modes based on the LLR- and CRC-driven reliability test. At low SNR, decoding is rarely reliable and the relay predominantly operates in SIR mode, causing the hybrid curve to tent with the SIR-only baseline. As the SNR increases, a growing fraction of frames satisfy the decoding reliability condition and activate DF relaying, while unreliable frames are still forwarded using SIR. This selective operation allows the hybrid scheme to outperform both DF-only and SIR-only relaying in the mid-SNR region by exploiting reliable DF opportunities while avoiding error propagation. At high SNR, decoding becomes almost always correct and the hybrid scheme converges to DF-only performance. The exact numerical outage results are in excellent agreement with the Monte-Carlo simulations across the entire SNR range, while the upper-bound-based

approximation also closely follows the simulation results, except for a slight mismatch observed in the low-SNR region. This confirms the accuracy of the derived outage expressions and supports the effectiveness of the proposed HDFSIR relaying strategy over mixed Rician-Nakagami fading channels.

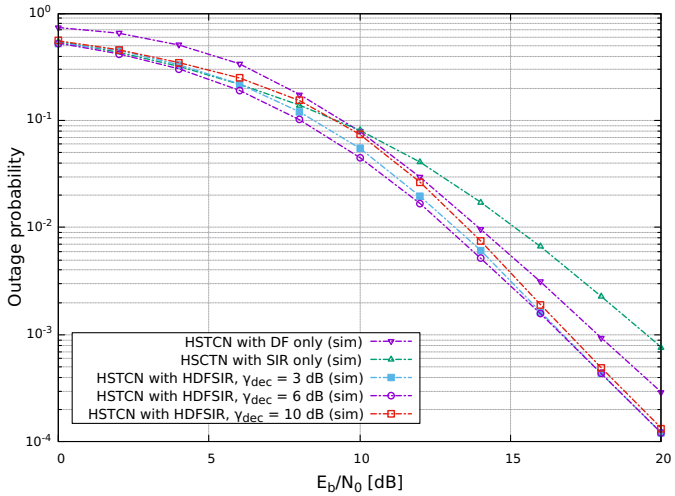


Fig. 4 Effect of DF Decision Threshold γ_{dec}. Outage probability performance of the HSTCN versus E_b/N_0 for three DF decision thresholds: a low threshold ($\gamma_{\text{dec}} = 3$ dB), a middle threshold ($\gamma_{\text{dec}} = 6$ dB) and a high threshold ($\gamma_{\text{dec}} = 10$ dB).

Fig. 4 highlights the impact of the decoding-reliability threshold on the HDFSIR scheme. Three decoding-reliability thresholds were evaluated to assess their impact on the outage performance of the HDFSIR relaying scheme. For a low decoding-reliability threshold (e.g., $\gamma_{\text{dec}} = 6$ dB), DF is activated more frequently whenever the CRC check is successful. While CRC verification prevents forwarding of incorrectly decoded frames, DF operation under marginal reliability conditions may still be suboptimal due to limited relay-destination link quality, leading to a higher outage probability than that obtained with a more conservative threshold that favors SIR in borderline regimes. When the threshold is increased to a moderate value (e.g., $\gamma_{\text{dec}} = 6$ dB), DF is mainly triggered in genuinely reliable decoding situations, whereas frames with doubtful reliability fall back to SIR. In this regime the hybrid scheme benefits simultaneously from the diversity gain of DF in good conditions and the robustness of SIR when DF is unreliable, which yields the lowest outage probability. For a high threshold (e.g., $\gamma_{\text{dec}} = 10$ dB), DF activation becomes rare and the relay relies predominantly on SIR, even when DF could have been used safely. The outage probability therefore increases again and approaches the SIR-only performance, since the potential DF diversity advantage is largely forfeited. At high SNR, relay decoding becomes almost always reliable, so all considered decoding-reliability thresholds are satisfied and DF is consistently selected regardless of γ_{dec}. Consequently, SIR is rarely invoked and

the HDFSIR scheme reduces to conventional DF relaying, causing the corresponding curves to merge in the high-SNR regime.

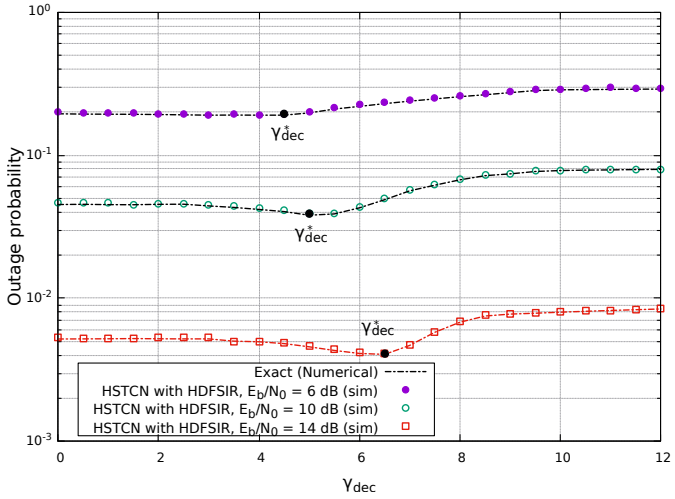


Fig. 5 Outage probability performance of the HSTCN versus the decoding-reliability threshold γ_{dec} for the proposed HDFSIR relaying scheme.

Fig. 5 illustrates the outage probability performance of the HSTCN with HDFSIR relaying scheme as a function of the decoding-reliability threshold γ_{dec}. Results are shown for fixed average SNRs (6, 10, and 14 dB). The curve exhibits a uni-modal behavior with a distinct minimum $\gamma^{\star}_{\text{dec}}$, representing the best trade-off between erroneous DF activation and overly conservative SIR operation. When γ_{dec} is set to a very low value, the relay frequently selects the DF mode even when its decoding quality is poor, which leads to a high outage probability due to error propagation. As γ_{dec} increases to a moderate or near-optimal level, incorrect DF activations are significantly reduced while correct DF decisions still occur frequently. Consequently, the outage probability decreases and reaches its minimum at the optimal threshold $\gamma^{\star}_{\text{dec}}$. However, when γ_{dec} becomes excessively high, the relay becomes overly conservative and relies predominantly on SIR, thereby missing beneficial DF opportunities. In this region, the outage probability rises again and approaches the SIR-only performance. It is also observed that for very low or very high average SNR values, the sensitivity to the threshold diminishes: at low SNR the DF mode is rarely helpful regardless of the threshold, whereas at high SNR decoding succeeds almost always, making the choice of γ_{dec} less influential. This explains the flattening of the outage curves at the two extremes of the SNR range.

Fig. 6 illustrates the average number of SISO iterations per frame versus average SNR per bit for DF-only, SIR-only, and the proposed HDFSIR relaying scheme. The average computational complexity results reflect the proposed LLR- and CRC-ased switching mechanism. In DF-only relaying, iterative decoding is performed until CRC

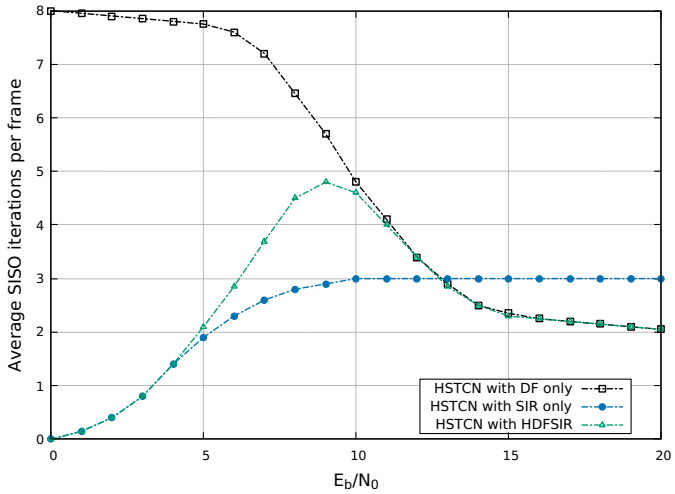


Fig. 6 Average computational complexity per frame. Average number of SISO iterations per frame versus average SNR for DF-only, SIR-only, and the proposed HDFSIR relaying scheme.

success or the maximum iteration limit, leading to a high average number of iterations at low SNR and a decreasing complexity at high SNR due to early stopping. In SIR-only relaying, decoding is restricted to a small fixed number of iterations (3 iterations in this experiment), while frames with very low LLR reliability are processed without iterations, resulting in low SNR-independent complexity. The HDFSIR scheme combines these behaviors and exhibits a characteristic "hump" around the decoding transition region (approximately ~ 8 dB). At low SNR, most frames fall into the zero-iteration region and the average complexity is close to zero. In the mid-SNR range, truncated SIR and occasional DF decoding are activated, increasing the average number of iterations. At high SNR, DF decoding dominates but converges rapidly due to CRC-based early stopping, causing the hybrid complexity to decrease again and approach the DF asymptote. This confirms that the proposed scheme significantly reduces computational load in unreliable conditions while preserving DF performance when decoding becomes reliable.

Fig. 7 illustrates the SER performance of the proposed HDFSIR relaying scheme for BPSK, QPSK and 16-QAM modulations. For BPSK, the HDFSIR scheme exhibits the lowest SER and the steepest slope, operating in an SIR-dominated regime at low SNR and progressively converging to DF behavior as relay decoding becomes reliable. The same hybrid transition is preserved for QPSK and 16-QAM constellations, with consistent modulation-dependent SER ordering and identical diversity trends.

The analytical SER curves are obtained from the proposed MGF-based formulation using the upper-bound approximation of the SIR link. As a result, a slight mismatch with the Monte-Carlo simulations is observed in the low-SNR region, where the bound is less tight. However, the analytical and simulated curves closely coincide in the medium- and high-SNR regimes, confirming that the proposed approximation

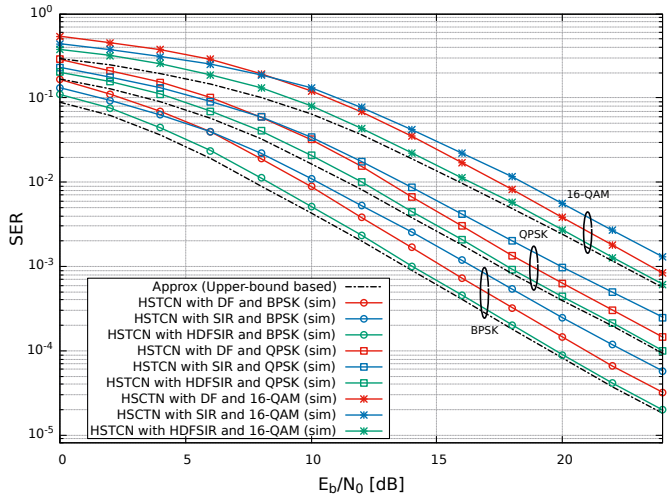


Fig. 7 SER performance of the proposed HSTCN versus average SNR for BPSK, QPSK, and 16-QAM modulations under the HDFSIR relaying protocol. Dashed curves denote analytical SER results obtained from the MGF-based formulation using the upper-bound approximation.

accurately captures the HDFSIR switching behavior and the impact of modulation order on the end-to-end error performance.

7 Conclusion

This paper has proposed and analyzed a HDFSIR strategy for coded hybrid satellite-terrestrial cooperative networks, where the S→R and S→D links undergo Rician fading and the R→D link follows a Nakagami-m model. A key contribution of this work is the development of a reliability-driven switching mechanism in which DF is invoked only when relay decoding is both successful and reliable, while unreliable frames are forwarded using SIR. This enables the relay to exploit DF whenever it is beneficial, while effectively avoiding DF error propagation. Another important contribution lies in the derivation of tractable statistical soft-symbol models that allow closed-form and semi-closed-form expressions for the outage probability, as well as approximate SER expressions, to be obtained under the considered mixed Rician-Nakagami fading channels.

Analytical and simulation results demonstrate that the proposed HDFSIR scheme achieves a clear performance advantage over conventional DF-only and SIR-only relaying. In particular, the hybrid strategy behaves as SIR in the low-SNR region, where DF decoding is unreliable, and converges to DF performance at high SNR, where decoding becomes almost always correct, while outperforming both schemes in the mid-SNR region through selective DF activation. From an implementation standpoint, the proposed HDFSIR scheme is readily deployable, as the switching decision relies on CRC outcomes and decoder-generated LLRs already available at the relay. In addition, SIR can be implemented with a limited number of SISO iterations, enabling

a favorable performance-complexity trade-off in practical satellite-terrestrial systems. As a result, the proposed framework provides not only improved reliability, but also reduced average processing complexity compared with DF-only relaying.

Overall, the results indicate that the HDFSIR relaying architecture constitutes a practical, analytically tractable, and low-complexity solution for future hybrid satellite-terrestrial networks, particularly in the context of emerging non-terrestrial 6G communication systems.

Statements and Declarations

Funding

No funding was received for conducting this study or for the preparation and publication of this manuscript.

Competing Interests

The author declares that there are no competing interests.

References

[1] J. Zhang, Y. Liu, L. Lv, N. Cheng, T. Q. S. Quek, and J. Wang, "Hybrid satellite-terrestrial networks toward 6G: Key technologies, opportunities, and challenges," *IEEE Wireless Commun.*, vol. 29, no. 4, pp. 74–81, Aug. 2022, doi: 10.1109/MWC.001.2100613.

[2] S. Dang, O. Amin, B. Shihada, and M.-S. Alouini, "Space-air-ground integrated networks: A survey and future challenges," *IEEE Commun. Surveys Tuts.*, vol. 23, no. 4, pp. 2134–2167, 4th Quart., 2021, doi: 10.1109/COMST.2021.3092282.

[3] M. Lin, K. An, J. Ouyang, T. Liang, and G. Zheng, "Performance analysis of integrated satellite-terrestrial networks with adaptive relaying," *IEEE Trans. Veh. Technol.*, vol. 72, no. 1, pp. 101–116, Jan. 2023, doi: 10.1109/TVT.2022.3214835.

[4] S. Sreng, B. Escrig, and M. L. Boucheret, "Exact outage probability of a hybrid satellite-terrestrial cooperative system with best relay selection," in *Proc. IEEE Int. Conf. Commun. (ICC)*, Budapest, Hungary, Jun. 2013, pp. 4520–4524, doi: 10.1109/ICC.2013.6655243.

[5] X. Wang, H. Zhang, and Z. Hou, "Performance analysis of multi-satellite hybrid satellite-terrestrial relay networks," *J. Earth Syst. Sci.*, vol. 131, no. 4, Art. no. 217, 2022, doi: 10.1007/s12040-022-01968-9.

[6] D. S. Ahn, S. Kim, H. W. Kim, and D. C. Park, "A cooperative transmit diversity scheme for mobile satellite broadcasting systems," *Int. J. Satellite Commun. Netw.*, vol. 28, no. 5–6, pp. 352–368, 2010, doi: 10.1002/sat.958.

[7] S. Kim, "Evaluation of cooperative techniques for hybrid/integrated satellite systems," in *Proc. IEEE Int. Conf. Commun. (ICC)*, Kyoto, Japan, Jun. 2011, pp. 1–5, doi: 10.1109/ICC.2011.5962678.

[8] K. An, M. Lin, J. Ouyang, Y. Huang, and G. Zheng, "Symbol error analysis of hybrid satellite-terrestrial cooperative networks with cochannel interference," *IEEE Commun. Lett.*, vol. 18, no. 11, pp. 1947–1950, Nov. 2014, doi: 10.1109/LCOMM.2014.2359975.

[9] K. An, M. Lin, and T. Liang, "On the performance of multi-user hybrid satellite-terrestrial relay networks with opportunistic scheduling," *IEEE Commun. Lett.*, vol. 19, no. 10, pp. 1722–1725, Oct. 2015, doi: 10.1109/LCOMM.2015.2463741.

[10] Z. Zhao, X. Zhang, W. Liu, H. Li, and D. Zhang, "Performance analysis of the hybrid satellite-terrestrial relay network with opportunistic scheduling over generalized fading channels," *IEEE Trans. Veh. Technol.*, vol. 71, no. 3, pp. 2914–2924, Mar. 2022, doi: 10.1109/TVT.2022.3147863.

[11] Q. Zhou, L. Yang, and R. D. Zhang, "Performance analysis of hybrid DF/AF relaying networks with energy harvesting," *IEEE Trans. Wireless Commun.*, vol. 22, no. 5, pp. 3201–3215, May 2023, doi: 10.1109/TWC.2023.3255451.

[12] L. Wang, S. Lin, and H. Wu, "Hybrid relaying strategy in wireless energy harvesting networks: A DF and AF approach," *IEEE Access*, vol. 11, pp. 26589–26601, 2023.

[13] Y. Liu, W. Zhao, and H. Tang, "Performance analysis of hybrid DF/AF relaying with distributed space-time coding," *IEEE Trans. Commun.*, vol. 71, no. 2, pp. 1245–1259, Feb. 2023.

[14] X. Wu, J. Li, and Y. Huang, "Cooperative strategies in hybrid DF/AF relaying systems with distributed space-time coding," *IEEE Trans. Wireless Commun.*, vol. 22, no. 8, pp. 4967–4979, Aug. 2023.

[15] L. Tang and M. Zhao, "Efficient protocols for hybrid DF/AF relaying and distributed space-time coding," *IEEE Access*, vol. 10, pp. 83985–83995, 2022.

[16] K. An, M. Lin, and T. Liang, "Performance analysis of multi-antenna hybrid satellite-terrestrial relay networks in the presence of interference," *IEEE Trans. Commun.*, vol. 63, no. 11, pp. 4390–4404, Nov. 2015, doi: 10.1109/TCOMM.2015.2472484.

[17] P. Weitkemper, D. Wübben, V. Kühn, and K. D. Kammeyer, "Soft-information relaying for wireless networks with error-prone source-relay link," in *Proc. 7th Int. ITG Conf. Source Channel Coding (SCC)*, Ulm, Germany, Jan. 2008.

[18] A. Abdi and M. Kaveh, "K distribution: An appropriate model for fading in high-frequency and satellite channels," *IEEE Trans. Commun.*, vol. 51, no. 3, pp. 300–303, Mar. 2003, doi: 10.1109/TCOMM.2003.809789.

[19] V. Karas and A. D. Panagopoulos, "Statistical modeling of shadowed Rician fading for land mobile satellite systems," *IEEE Trans. Veh. Technol.*, vol. 55, no. 1, pp. 1–11, Jan. 2006, doi: 10.1109/TVT.2005.861192.

[20] S. Parthasarathy, M. Sellathurai, and C. B. Papadias, "Shadowed-Rician modeling for land mobile satellite channels: A review," *IEEE Access*, vol. 8, pp. 112158–112178, 2020, doi: 10.1109/ACCESS.2020.3002765.

[21] Z. Zhao, X. Zhang, W. Liu, H. Li, and D. Zhang, "Symbol error analysis of amplify-and-forward based multiuser hybrid satellite-terrestrial relay network," *IEEE Wireless Commun. Lett.*, vol. 10, no. 10, pp. 2279–2283, Oct. 2021, doi: 10.1109/LWC.2021.3103457.

[22] S. Papaharalabos, P. Sweeney, and B. G. Evans, "SISO algorithms based on Max-Log-MAP and Log-MAP turbo decoding," *IET Commun.*, vol. 1, no. 1, pp. 49–54, Feb. 2007, doi: 10.1049/iet-com:20060090.

[23] S. S. Shapiro and M. B. Wilk, "An analysis of variance test for normality (complete samples)," *Biometrika*, vol. 52, no. 3–4, pp. 591–611, 1965, doi: 10.1093/biomet/52.3-4.591.

[24] E. H. Cui, Y. Li, and Z. Liu, "The Kolmogorov-Smirnov statistic revisited," arXiv:2503.11673, 2025.

[25] S. Chaoui, O. Alruwaili, F. Alserhani, and H. Harrouch, "Hybrid DF and SIR forwarding strategy in conventional and distributed Alamouti space-time coded cooperative networks," *Comput. Model. Eng. Sci.*, vol. 142, no. 2, pp. 1933–1954, 2025, doi: 10.32604/cmes.2025.059346.

[26] G. Caire, G. Taricco, and E. Biglieri, "Bit-interleaved coded modulation," *IEEE Trans. Inf. Theory*, vol. 44, no. 3, pp. 927–946, May 1998, doi: 10.1109/18.669123.

[27] J. G. Proakis and M. Salehi, *Digital Communications*, 5th ed. New York, NY, USA: McGraw-Hill, 2007.

[28] B. Sklar, *Digital Communications: Fundamentals and Applications*, 2nd ed. Upper Saddle River, NJ, USA: Prentice Hall, 2001.

[29] M. C. Valenti and S. B. Wicker, "Soft-input soft-output algorithms for decoding turbo codes," in *Proc. 39th Allerton Conf. Commun., Control, Comput.*, Monticello, IL, USA, Oct. 2001.

[30] A. Guillén i Fàbregas and A. Martinez, "Bit-interleaved coded modulation," *Found. Trends Commun. Inf. Theory*, vol. 5, no. 1–2, pp. 1–153, 2008, doi: 10.1561/0100000006.

[31] H. Lin and R. Schober, "Soft-information relaying for coded wireless relay networks," *IEEE Trans. Commun.*, vol. 55, no. 12, pp. 2297–2306, Dec. 2007, doi: 10.1109/TCOMM.2007.908556.

[32] M. K. Simon and M.-S. Alouini, *Digital Communication over Fading Channels*, 2nd ed. New York, NY, USA: Wiley, 2005.